Introduction of a Chemical Constraint in a Short Peptide Derived from Human Acidic Fibroblast Growth Factor Elicits Mitogenic Structural Determinants

Sumika Kiyota,[§] Lorella Franzoni,[‡] Giuseppe Nicastro,[‡] Arianna Benedetti,[‡] Sérgio Oyama, Jr.,[§,†] Wládia Viviani,[§] Angelo G. Gambarini,[§] Alberto Spisni,[‡,†] and M. Terêsa M. Miranda*[,§]

Department of Biochemistry, Institute of Chemistry, University of São Paulo, P.O. Box 26077, 05513-970, São Paulo, Brazil, and Department of Experimental Medicine, Section on Chemistry and Structural Biochemistry, University of Parma, 43100, Parma, Italy, and Centre for Molecular and Structural Biology, CeBiME, LNLS, 13084-971, Campinas, Brazil

Received December 3, 2002

Fibroblast growth factors (FGFs) are regulatory proteins associated with a number of physiological and pathological states. On the basis of data suggesting a functional role for specific regions of human acidic FGF (aFGF), a linear peptide encompassing residues 99−108 (peptide**1**) and its cyclic analogue (peptide **2**) were synthesized and their functional and structural features were investigated. While peptide **1** is inactive on Balb/c 3T3 fibroblasts, peptide **2** is mitogenic with ED_{50} of ∼50 μM. Moreover, peptide **1** is not able to inhibit the binding of human aFGF to cellular receptors whereas peptide **2** exhibits significant inhibitory activity. The NMR-derived solution conformers indicated the presence, only in peptide **2**, of structural elements that we believe are related to its ability to emulate the biological activity of the native protein. These results suggest that the expression of mitogenic activity in short peptides, besides the presence of specific amino acids, requires the existence of stable structural features. In addition, they indicate that the introduction of chemical restraints in peptides can provide novel possibilities for the development of receptor agonists or antagonists.

Introduction

Fibroblast growth factors (FGFs) constitute a large family of heparin-binding proteins whose receptors (FGFRs) are transmembrane tyrosine kinases.[1] The expression of these growth factors is associated with cell proliferation, division, embryonic differentiation and morphogenesis as well as with several physiological and pathological states such as angiogenesis, wound healing, tumor growth, and metastasis.[2,3] These proteins have also been associated with some pathologies such as rheumatoid arthritis, diabetic retinopathy, and arteriosclerosis.[4]

It is well-known that the binding of FGFs to their receptors initiates a signal transduction pathway that requires receptor dimerization and trans-autophosphorylation of the tyrosine kinase domains, thus triggering mitogenesis as cellular response.[5,6]

Experimental observations suggest that heparan sulfate (HS), a proteoglycan widely distributed in cell surfaces and extracellular matrixes of many tissues, mediates the formation of the active FGF−FGFR complex.[2,7] Indeed, many authors have reported that HS provides for FGFs storage and regulates the mechanism of their release from cell surfaces.[8,9] Additionally, the binding of the FGFs to heparin (HEP), structurally related to HS, appears to stabilize the conformation of these proteins and to diminish their in vitro inactivation.[10−13]

These observations explain the effort to identify the location of the FGF−HS binding site and to determine the role of that glycosaminoglycan in the FGF−FGFR binding process. As a result, a few models of the FGF−FGFR−HEP complex have been proposed. They are characterized by a variable stoichiometry of the active complex: 1:2:1 FGF−FGFR−HEP/HS;[14−16] 2:2:1 or 2:2:2 FGF−FGFR−HEP/HS.[7,17,19]

The analysis of the crystalline dimeric complex formed by human aFGF and the two extracellular domains of the isoform 2 of FGFR (FGFR-2) revealed that the receptor sequence ^{161}KMEKRLHAVPAANTVKFR^{178}, which is involved in the primary binding to the protein, is part of the A′ strand.[20,21] On the other hand, the residues of human aFGF present at the protein−receptor interface belong to the β1, β2, β9, and β12 strands, to the β1/β2 turn and β3/β4 and β10/β11 loops, and to the C-terminus.[20] Interestingly, the segment ^{97}YISKKHAEKNWFVGLKKNGSCKRGPRTHYGQK-AILF^{132} [numbered according to Blaber and co-workers[22]], which in human aFGF encompasses the β9/β10 loop and the N-terminus of β10[23], has been considered important in the process of recognition of the FGFR isoforms.[22] Similarly, in the case of human basic fibroblast growth factor (bFGF), sequence 97−132 belongs to a region important for the selective recognition of the specific FGFR isoform for receptor dimerization and for the binding of HEP.[15,24]

Finally, the analysis of crystalline heteropentameric assembly of human aFGF, FGFR-2, and HEP (2:2:1) allowed the identification of the amino acid residues involved in the contact between these components and indicated that many of them are from segment 161−178 of the receptor and segment 97−132 of the agonist.[25]

In an attempt to devise new short peptides that could mimic the biological activity of human aFGF, we designed a peptide encompassing residues 99−108,

* To whom correspondence should be addressed. Phone: 11-3091-3855. Fax: 11-3815-5579. E-mail: mtmirand@iq.usp.br.
[§] University of São Paulo.
[†] Centre for Molecular and Structural Biology.
[‡] University of Parma.

10.1021/jm020543e CCC: $25.00
Published on Web 05/08/2003

Table 1. Peptides Purification and Biological Characterization[a]

peptide	purification data: mass of crude peptide (mg)	purification data: yield (%)	RP-HPLC purity TFA system/ TEAP system (%/%)	MALDI-TOF MS obsd (calcd) (*m*/*z*)	biological activity[b]: ED_{50} (μM)	biological activity[b]: ID_{50} (μM)
1	50	53	96/90	1316.1 (1316.5)	inactive	>1000
2	90	50	99/92	1363.0 (1362.8)	~50	~30
3[c]					10−20[c]	30−50[c]

[a] Amino acid analyses of peptides **1** and **2** gave the expected amino acids in the correct molar proportion. [b] Tested in the peptide concentration range of 0−200 μM. [c] The biological activity of peptide Ac-WFVGLKKNGSSKRGPRT-NH_2, studied previously,[26] is used as a reference for the other peptides.

SKKHAEKNWF-NH_2 (peptide **1**), that contains the motif Trp^{107}-Phe^{108} suggested to be important for the activity of mitogenic peptides derived from this protein.[26] Since in the crystal structure the region Tyr^{97}-Phe^{132} contains the segment Ser^{99}-Ala^{103} that forms a bend,[22,27] where the distance between Ser^{99} Cα and Ala^{103} Cα is about 5.5 Å, we synthesized peptide **2**, Ac-CKKHCEKNWF-NH_2, also an analogue of peptide **1** where that bend was stabilized via a sulfur bridge. Here, we report their chemical, biochemical, and structural characterization.

Results

Peptide Synthesis and Purification. Stepwise solid-phase synthesis of peptides **1** and **2** was straightforward. Some difficulties were encountered during the purification of peptide **2** because the synthetic crude material contained a major byproduct that coeluted with it. The use of two distinct solvent systems (TFA and TEAP), manual fraction collection, and a check of each fraction under isocratic conditions resolved this problem, and peptide **2** was isolated at a purity higher than 90%. Characterization of the byproduct (data not shown) revealed that it was a cyclized analogue lacking asparagine: Ac-(cyclo 1−5)CKKHCEKWF-NH_2. Characterization by amino acid analysis and mass spectrometry of the purified peptides confirmed their purity and chemical identity (Table 1).

Biological Characterization. As shown in Figure 1, peptide **1** turned out to be unable to promote mitogenic response when added to Balb/c 3T3 fibroblast culture, clone A31, at concentrations up to 200 μM. Peptide **2** instead elicits a mitogenic response comparable to that exhibited by a peptide encompassing residues 107−123 of human aFGF, Ac-WFVGLKKNG-SSKRGPRT-NH_2, peptide **3**.[26] Table 1 shows the ED_{50} obtained for peptides **1**−**3**.

When the affinity of the peptides for HEP was tested, while the entire protein is eluted with 1.5 M NaCl, peptides **1** and **2** require 0.41 and 0.39 M NaCl, respectively.

Finally, the dose−response plots indicated that peptide **2** is able to inhibit the binding of human aFGF with an ID_{50} of ~30 μM, while peptide **1** is inactive, showing an ID_{50} greater than 1 mM (Table 1).

Structural Characterization. The CD spectra at 20 °C in buffered aqueous solutions do not indicate a stable ordered secondary structure at any pH tested (Figure 2). In addition, the shape of the spectra is independent of peptide concentration, thus discarding the possibility of aggregate formation (data not shown).

In both cases, (Figure 3), upon addition of increasing amounts of MeOH, while the negative band shifts from 198 nm to longer wavelengths, a broad negative shoulder appears around 220 nm, suggesting the appearance of some elements of a secondary structure such as turns. A similar behavior is also observed with TFE (data not shown).

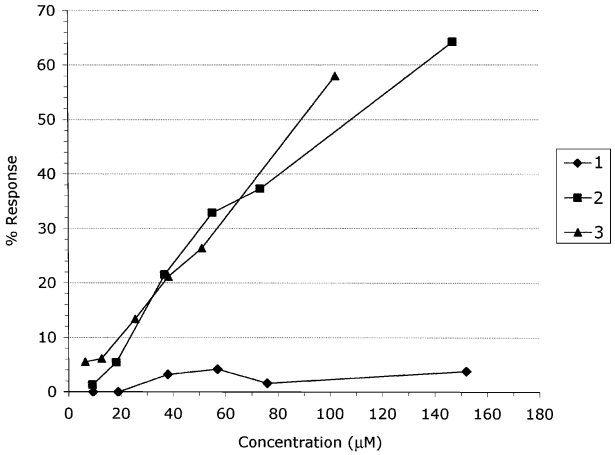

Figure 1. Effect of peptides **1**−**3** on the incorporation of [^{3}H-methyl]-thymidine by Balb/c 3T3 fibroblasts, clone A31. Cells were growth-arrested with low serum (1.0%) and incubated with 0−200 μM of each peptide in the presence of 5 μg/mL insulin. The percentage of response (% R) was calculated in the following way: the counts per min (cpm), obtained from each experimental well were subtracted from the basal count (no peptide additions) and divided by that obtained with addition of 10% FCS final concentration (also subtracted from the basal counts). The biological activity of peptide **3**[26] was used as a reference to evaluate the other peptides derived from human aFGF-1.

The complete sequence-specific NMR assignment of the two peptides was achieved according to established procedures.[28] The proton chemical shifts at 25 °C are reported in Table 2 for both molecules.

The qualitative analysis of the ROE connectivities suggests that the conformational features of the two peptides are significantly different. As summarized in Figure 4 (top), peptide **1** shows a single medium-range ROE. In contrast, 13 medium-range connectivities are observed in the case of peptide **2** (Figure 4, bottom).

For peptide **1**, only 49 nonredundant distance constraints (including 30 intraresidual and 18 sequential) have been used to compute its three-dimensional structures. Owing to the limited number of NMR constraints available, the entire molecule is poorly defined. Among the 50 final structures, only 9 could be selected on the basis of their lower residual distance and dihedral angle violations (less than 0.3 Å and 5°, respectively), as well as their lower energy, and they were used to represent a possible 3D structure of the peptide. As shown in Figure 5A, the superposition of the sequence Lys^2-Ala^5 (pairwise backbone rmsd of 0.45 ± 0.15 Å) suggests the

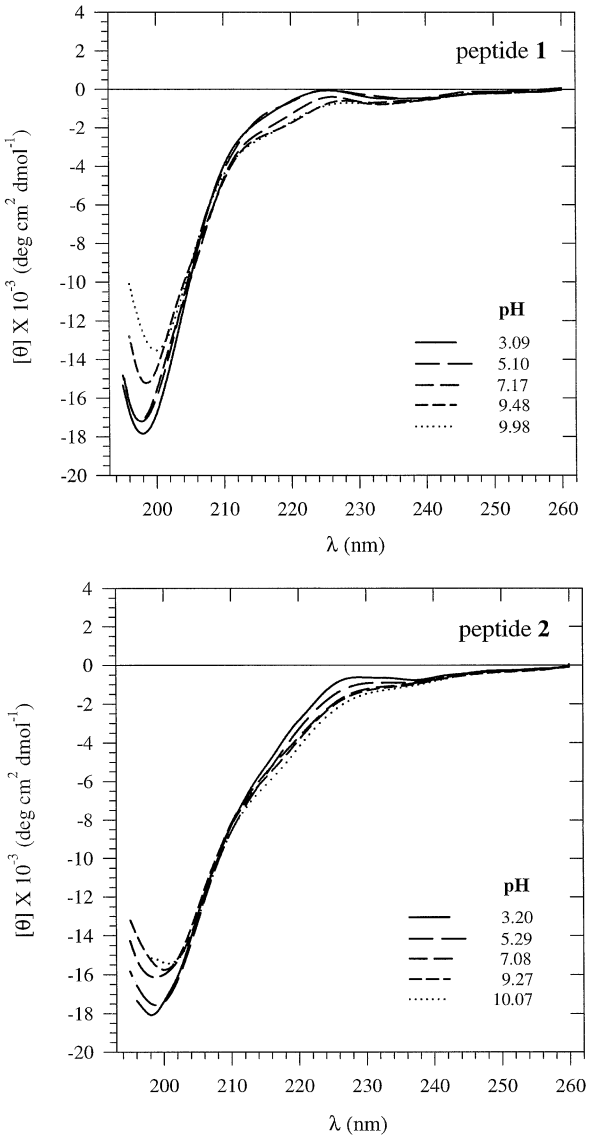

Figure 2. CD spectra of peptides **1** and **2** in buffered aqueous solutions at 20 °C as a function of pH.

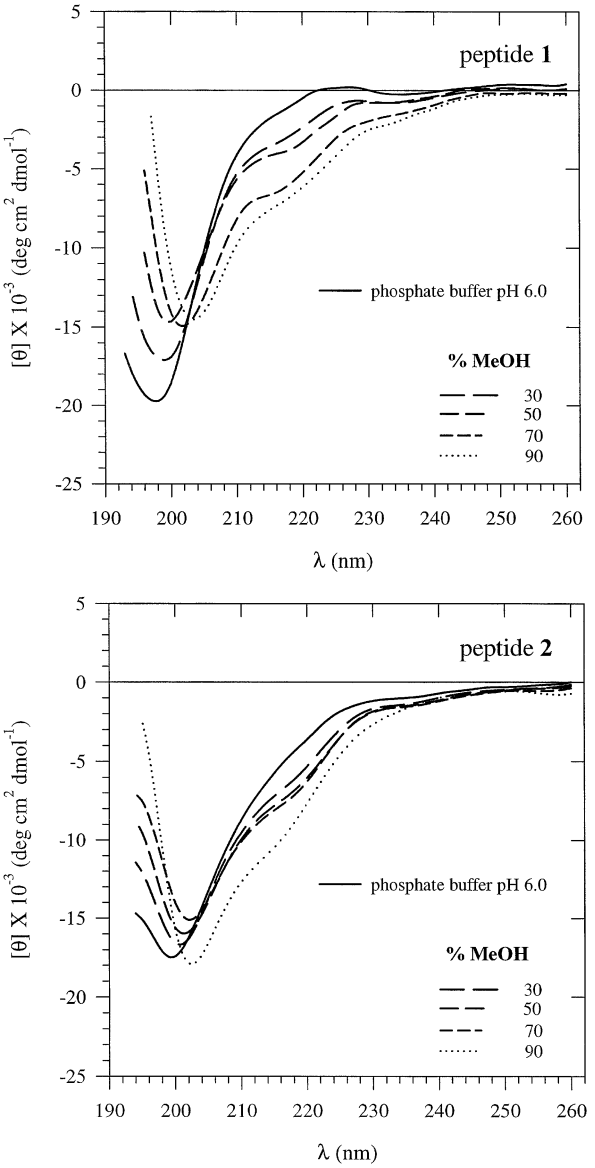

Figure 3. CD spectra of peptides **1** and **2** in 10 mM phosphate buffer (pH 6.0) at 20 °C as a function of increasing MeOH concentrations (% v/v).

presence of a "turnlike" motif. On the other hand, the C-terminus region does not acquire any preferred conformation.

In the case of peptide **2**, a significantly greater number of constraints (a total of 93, including 50 intraresidual and 30 sequential) has been used to compute its 3D structures. All the calculated conformers show no significant violations of any single distance constraint. As expected, all structures present a bend in the domain Cys^1-Cys^5 due to the disulfide bridge between these two residues. Figure 5B shows an ensemble of nine models that exhibit the best superposition of the backbone atoms in the domain Cys^1-Glu^6, pairwise rmsd = 0.66 ± 0.19 Å, and that can be considered representative of the structural motif in the N-terminus of peptide **2** in solution. The rmsd value slightly drops to 0.53 ± 0.15 Å when reducing the superposition to Lys^2-Glu^6. The average Cα−Cα distance between Cys^1 and Cys^5 is 4.4 Å.

Interestingly, the majority of the medium-range ROEs observed for peptide **2** involve the middle region and the C-terminus of the molecule (Figure 4, bottom), suggesting the occurrence of some structural elements in that domain. On the basis of the analysis of the ϕ and ψ dihedral angle distribution, it has been possible to divide the selected conformers into two subfamilies. The first one comprises 13 structures with the common characteristic of displaying a hydrogen bond between the backbone carbonyl of Glu^6 and the amide group of Trp^9 (Figure 6A). The backbone superposition in the region Cys^5-Phe^{10} gives an rmsd of 0.46 ± 0.21 Å, and according to the ROE pattern and to ϕ and ψ dihedral angles, a slightly distorted type-II β-turn spanning the residues Glu^6-Trp^9 can be identified.

In a second subfamily, again containing 13 conformers, the C-terminus of peptide **2** still folds to form a β-turn in the same Glu^6-Trp^9 region. Differently from the previous case, however, the Glu^6 CO points outside the turn, thus preventing the formation of the hydrogen bond with Trp^9 NH. Figure 6B shows this ensemble of structures that have been superposed in the region Cys^5-Phe^{10} with an rmsd of 0.49 ± 0.25 Å.

The finding that distinct local structural motifs are compatible with the same NOE and/or ROE pattern is

Table 2. ^{1}H NMR Chemical Shifts[a] (ppm) for Peptides **1** and **2** in Phosphate Buffer/CD_3OH (1:1, v/v), pH ~6, at 25 °C

residue	N_H	α_H	β_H	γ_H	others
			For Peptide **1**		
Ac					CH_3 1.90
Ser^1	8.22	4.35	3.85−3.77		
Lys^2	8.38	4.32	1.84−1.84	1.42	δ_H 1.67; ϵ_H 2.95
Lys^3	8.09	4.20	1.72−1.72	1.35	δ_H 1.65; ϵ_H 2.93
His^4	8.33	4.65	3.24−3.12		H^2 8.60; H^4 7.28
Ala^5	8.32	4.29	1.36		
Glu^6	8.23	4.35	1.91−2.06	2.40	
Lys^7	8.21	4.19	1.61−1.61	1.25	δ_H 1.51; ϵ_H 2.82; ϵ_{NH} 7.60
Asn^8	8.25	4.63	2.65−2.65		γ_{NH_2} 6.83−7.51
Trp^9	7.91	4.47	3.06−3.06		H^2 7.08; H^4 7.51; H^5 7.08; H^6 7.14; H^7 7.41; N^1H 10.16
Phe^{10}	7.71	4.45	2.81−2.94		δ_H 7.10; ϵ_H 7.27; ζ_H 7.24; term-NH_2 6.96
			For Peptide **2**		
Ac					CH_3 1.973
Cys^1	8.30	4.31	2.98, 3.13		
Lys^2	8.86	4.35	1.74, 1.85	1.39, 1.46	δ_H 1.65; ϵ_H 2.94; ϵ_{NH} 7.66
Lys^3	7.93	4.27	1.66	1.24	δ_H 1.62; ϵ_H 2.88
His^4	8.76	4.48	3.22, 3.29		H^2 8.56; H^4 7.22
Cys^5	8.29	4.57	2.79, 3.24		
Glu^6	8.65	4.19	1.93, 2.02	2.34	
Lys^7	8.23	4.15	1.62	1.26	δ_H 1.56; ϵ_H 2.83; ϵ_{NH} 7.61
Asn^8	8.20	4.58	2.64		γ_{NH_2} 6.83, 7.52
Trp^9	7.90	4.44	3.06, 3.04		H^2 7.06; H^4 7.49; H^5 7.05; H^6 7.13; H^7 7.39; N^1H 10.15
Phe^{10}	7.695	4.433	2.798, 2.945		δ_H 7.100; ϵ_H 7.263; ζ_H 7.230; term-NH_2 6.97

[a] Chemical shifts are relative to the water resonance located at 4.81 ppm.

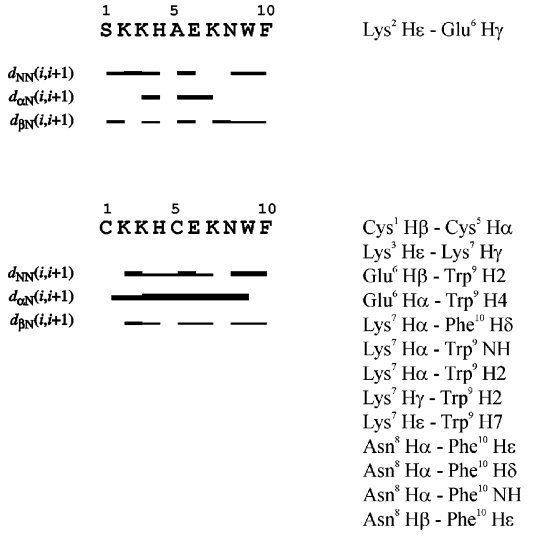

Figure 4. Sequential (left) and medium-range (right) ROEs of peptides **1** (top) and **2** (bottom). Spectra were collected in 10 mM phosphate buffer (pH 6.0)/CD_3OH (1:1 v/v) at 25 °C.

not surprising. In fact, in short peptides, a rigorous interpretation of NOEs is not possible because of the existence of multiple structures (conformational variability) and because of the absence of a unique correlation time for the molecule (segmental mobility). As a result, the identification of clusters of structures compatible with the experimental NOEs and exhibiting similar elements of the secondary structure turns out to be useful because it can provide a direct visualization of the molecular plasticity of the peptide.[29]

In summary, the results described above indicate that while the linear peptide exists mainly in an extended conformation and is inactive, the cyclized analogue acquires elements of secondary and tertiary structures that may be correlated to its biological activity.

Discussion

The study of synthetic peptides encompassing portions of proteins has turned into a supportive tool for understanding the molecular mechanisms associated with protein biological functions.[30−33] On the other hand, since short peptides are quite flexible, the introduction of chemical constraints is often mandatory to reduce

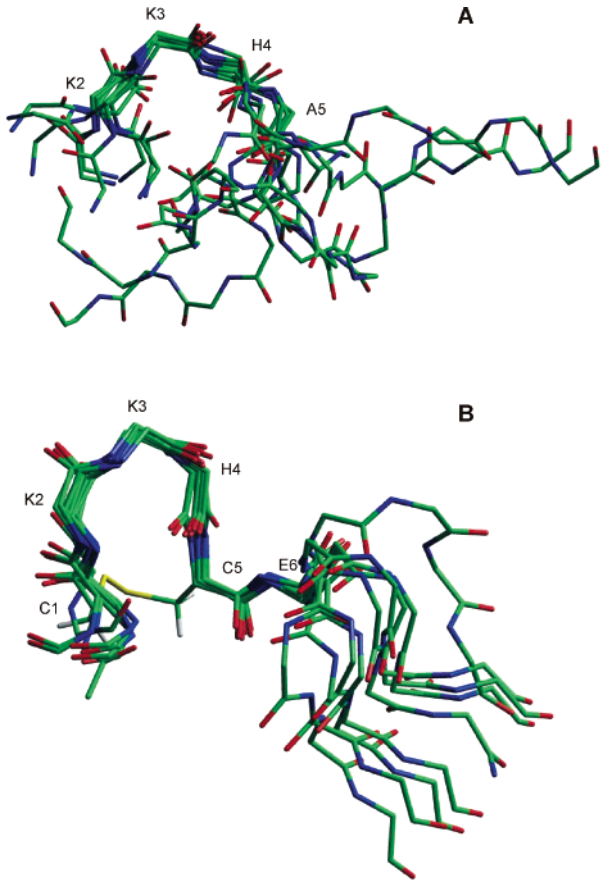

Figure 5. Selected NMR-derived solution structures of peptides **1** (A) and **2** (B) showing the structural motif present at the N-terminus. The superposition of the backbone atoms has been made for residues Lys^2-Ala^5 (rmsd of 0.45 ± 0.15 Å) and Cys^1-Glu^6 (rmsd of 0.66 ± 0.19 Å) for peptides **1** and **2**, respectively. In the case of peptide **2**, the disulfide bridge (Cys^1-Cys^5) is shown for only one structure.

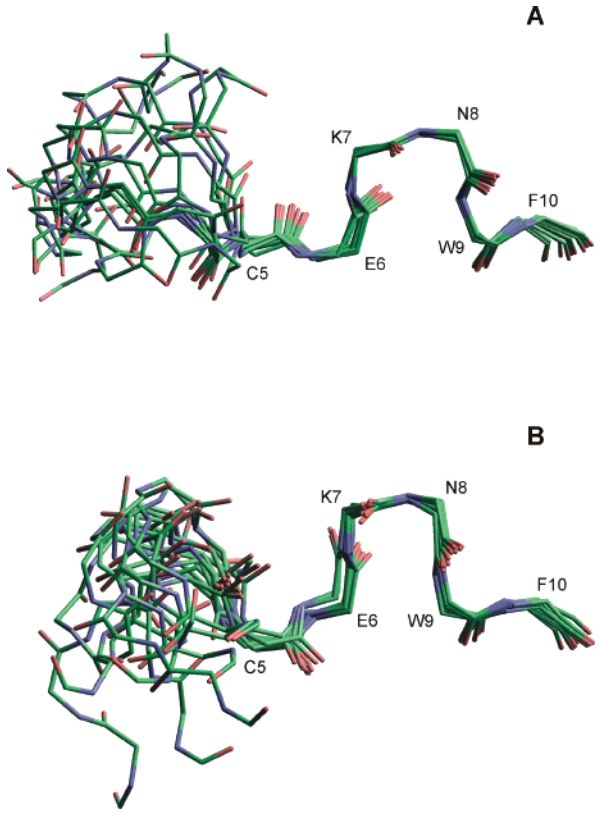

Figure 6. Selected NMR-derived solution structures of peptide **2** showing the structural motif present at the C-terminus. The superposition of the backbone atoms has been made in the domain Cys[5]-Phe[10] (part A shows an rmsd of 0.46 ± 0.21 Å; part B shows an rmsd of 0.49 ± 0.25 Å). The ensemble of structures shown in part A forms a slightly distorted type-II β-turn spanning residues Glu[6]-Trp[9], where the Glu[6] CO is hydrogen-bonded to Trp[9] NH. The conformers displayed in part B form a β-turn in the same domain, but Glu[6] CO points outward, preventing the formation of the hydrogen bond with Trp[9] NH.

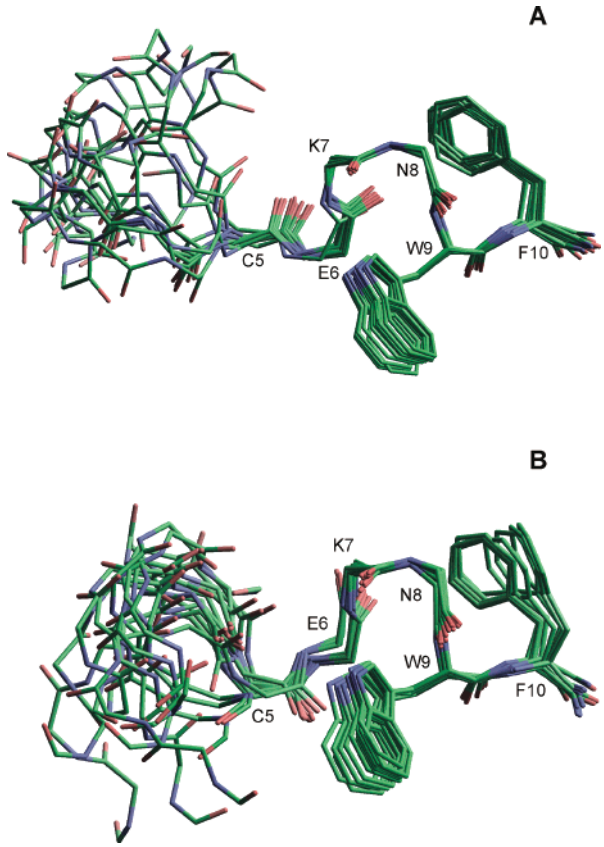

Figure 7. Comparison of the orientation of the Trp[9] and Phe[10] side chains in peptide **2**. Parts A and B show the same ensembles of structures presented in parts A and B of Figure 6, respectively, using a different rotation.

their conformational space and to better mimic protein functional motifs.[34−38]

Many authors, in an attempt to identify the FGF functional domains, have studied linear short peptides corresponding to portions of these regulatory proteins.[14,39−42] Nevertheless, a rational design of constrained active peptides encompassing regions of FGFs has not received much attention so far.

In the case of human aFGF, previous studies showed that while the synthetic peptides Ac-Y[97]ISKKHAEK[105]-NH_2 and Ac-G[110]LKKNGSSKRGPRT[123]-NH_2 were inactive on Balb/c 3T3 fibroblast culture, Ac-S[99]KKHAE-KNWFVGLKKN[114]-NH_2, Ac-N[106]WFVGLK[112]-NH_2, and Ac-WFVGLKKNGSSKRGPRT-NH_2 (peptide **3**) were mitogenic ($ED_{50} \approx 10-20\ \mu M$), able to inhibit the binding to the receptor of native aFGF ($ID_{50} \approx 30-200\ \mu M$), and capable of binding to a HEP−Sepharose column.[26]

The ineffectiveness of SKKHAEKNWF-NH_2 on Balb/c 3T3 fibroblasts, clone A31, however, clearly indicated that the primary sequence identity is not sufficient to guarantee their biological activity. On the other hand, the finding that peptide **1** did not exhibit any preferential conformation, with only a few models presenting a poorly defined bend at the N-terminus, pointed to the possible need of some stable secondary structure elements. Indeed, in peptide **2**, the disulfide bridge forces a bend in the N-terminus, with a Cys[1] Cα−Cys[5] Cα distance of 4.4 Å, (Figure 5B), that is reminiscent of the structural motif present in human aFGF.[22,27]

More than that, our data indicate that the presence of such a conformational restriction also promotes a structural organization of the C-terminal portion of peptide **2** (Figure 6), which contains the Trp-Phe motif, previously suggested by us[26] as important for the expression of the mitogenic activity of peptide **3** (see Table 1). In fact, a β-turn is stabilized in that region, and a number of medium-range ROEs involving the side chain protons of Trp[9] and Phe[10] (Figure 4, bottom) indicate that these side chains exhibit a preferential orientation evident in both subfamilies of structures (Figure 7).

Interestingly, this peptide exhibits clear mitogenic activity, though 10^4-fold less than that of the entire protein (Table 1). Another important functional feature of FGFs is the ability to bind to HEP via polar interactions using their positively charged residues.[10−14,17−19,42−45] Indeed, our results show that the activity of peptide **1** is unaffected by the presence of HEP in the cell culture medium. Nonetheless, they indicate that peptides **1** and **2** do interact with HEP in an elution experiment with a HEP−Sepharose column, though with an affinity weaker than that of the intact protein. Therefore, consistent with the observations of Ballinger and coworkers,[46] we interpret this low affinity for HEP as the result of their reduced molecular dimensions that allow only partial intermolecular interaction.

To verify whether the mitogenic activity of peptide **2** is the result of a possible interaction with FGFR and can be correlated to the one expressed by human aFGF, we tested its capability of inhibiting the binding of aFGF to Balb/c 3T3 fibroblast surface receptors. Differently from peptide **1**, peptide **2** exhibited clear inhibitory activity (Table 1), thus indicating that the chemical restraint elicits structural features that enable the peptide to interfere with the binding of aFGF to the receptors present in the cells tested.

To date, we have no direct experimental evidence that peptide **2** expresses its activity through the binding to an extracellular domain of the FGFR. Nevertheless, the fact that it inhibits the binding of aFGF is quite evocative of such a possibility. If we accept the idea that the peptide partially mimics the structure of a region of human aFGF, we may then hypothesize that it binds to the same receptor sites, in particular the ones formerly known as high-affinity or low-affinity receptor binding sites (regions 1 or 2, respectively).

Alternatively, it is conceivable that peptide **2** may be only a mimetic of the human aFGF binding surface. In fact, it contains structural determinants similar to those present in the "consensus binding sites"[47] as well as to those indicated as "hot spots" or "functional epitopes".[48] Under this assumption, peptide **2** would bind to other regions of FGFR, being able in any case to trigger the mitogenic response or to inhibit the binding of human aFGF.

In conclusion, we have shown that the introduction of an S−S bridge in a short peptide encompassing a portion of human aFGF can affect its structure, conferring to the peptide the ability to partially mimic the mitogenic activity of the whole protein. Hence, we believe this work provides new insights to the rational engineering of compounds that have the potential to efficiently agonize or antagonize the important biological functions of the FGF family members. To the best of our knowledge, peptide **2** is the first chemically constrained mitogenic peptide, related to human aFGF, to be reported.

Experimental Section

Peptide Design and Synthesis. Peptides **1** and **2** have been designed on the basis of a number of results from our group and other laboratories.[14,15−20,22,23,26,49−53] They were manually synthesized using the stepwise solid-phase method, t-Boc strategy, and customized protocols.[54] Both molecules were N-terminal-acetylated and C-terminal-amidated. The peptide chain was built up on methylbenzhydrylamine resin (MBHA) using mostly 1 M diisopropylcarbodiimide (DIC) in dichloromethane (DCM) as coupling reagent. The incorporation of the asparagine residue was accomplished in *N*,*N*-dimethylformamide (DMF) in the presence of a mixture of 1 M DIC/DCM and 1-hydroxybenzotriazole (HOBt) in equimolar amounts. Full deprotection and simultaneous cleavage from MBHA were carried out in anhydrous hydrogen fluoride containing 1% anisole, peptide **1**, or 1% anisole/dimethyl sulfide, peptide **2**. The crude peptides were precipitated in diisopropyl ether and extracted with 0.1% trifluoroacetic acid (TFA) and 60% acetonitrile (ACN)/0.1% TFA.

Peptide **1** was lyophilized to give the solid crude material. Cyclization of peptide **2** was carried out immediately after cleavage from the resin and full deprotection. The solution containing the crude material was diluted with deionized water, and the pH of the resulting solution was adjusted to 7.5−8.0 with 50% ammonium hydroxide solution.[55] Air oxidation of the thiol groups was monitored by analytical RP-HPLC on a Vydac C_{18} column (5 μm, 300 Å, 0.46 cm × 25.0 cm) under the following experimental conditions: triethylammonium phosphate (TEAP) as solvent A, 60% acetonitrile/(solvent A) as solvent B, gradient from 5% to 95% solvent B in 30 min, wavelength of 220 nm, flow rate of 1 mL/min. Once the disulfide bridge was formed, the pH of the solution was adjusted to 5.0 and the solvent was eliminated under high vacuum. The remaining solid product was lyophilized.

Peptide Purification and Characterization. Crude lyophilized peptides were purified by RP-HPLC in two steps using a Beckman System Gold semipreparative equipment coupled to a C_{18} column (Vydac, 5 μm, 300 Å, 2.2 cm × 25.0 cm) and a flow rate of 10 mL/min. Each step required a selected solvent system and a specific linear gradient. Step 1 had the following parameters: solvent A, TEAP, pH 2.5; solvent B, 60% acetonitrile/(solvent A); gradient from 20% to 45% solvent B in 40 min for peptide **1** and from 20% to 35% solvent B in 40 min for peptide **2**. Step 2 had the following parameters: solvent A, 0,1% TFA; solvent B, 60% acetonitrile/(solvent A); gradient from 25% to 45% solvent B in 40 min for both peptides. Absorption was measured at 220 nm.

Each of the peptide fractions collected was analyzed on a Vydac C_{18} column (5 μm, 300 Å, 0.46 cm × 25.0 cm) coupled to an LDC analytical HPLC system (Thermo Separation Products; composed of a ConstaMetric 3500 pump, a ConstaMetric 3200 pump, a UV−vis spectrometer model 3100 detector, a Rheodyne model 7125 injector, and a Waters 745B integrator) using TEAP cited above as the solvent system with the following parameters: flow rate of 1 mL/min, wavelength of 220 nm, and a linear gradient from 25% to 45% solvent B in 10 min.[56]

Peptide purity was measured by analytical RP-HPLC using the TFA and TEAP solvent systems mentioned above with a flow rate of 1 mL/min, wavelength of 220 nm, and the following gradients: from 25% to 45% solvent B in 20 min for peptide **1** and from 20% to 40% solvent B in 20 min for peptide **2**. The values obtained were 96% (TFA) and 90% (TEAP) for peptide **1** and 99% (TFA) and 92% (TEAP) for peptide **2**.

Peptide identity was determined by amino acid analysis and mass spectrometry. Briefly, the purified peptides were hydrolyzed for 24 h at 110 °C in the presence of 6 N HCl vapor and phenol on a Waters Pico-Tag workstation. After total evaporation of the solvent, the hydrolyzed samples were dissolved in buffer and analyzed on a Beckman automatic amino acid analyzer, model 7300. Comparatively, a sample of the intact molecule was injected and analyzed in a MALDI-TOF mass spectrometer (Bruker Daltonics, Inc.) using α-cyano-4-hydroxycinnamic acid as the matrix.

Peptide Mitogenic Activity. The mitogenic activity of the peptides was evaluated by measuring the amount of tritiated thymidine incorporated into the DNA of Balb/c 3T3 fibroblasts, clone A31. Briefly, cells were seeded into 24-well plates at a concentration of about 50 000 cells/well and grown to near-confluence in Dulbecco's modified Eagle's medium (DMEM) supplemented with 10% fetal calf serum (FCS). Subconfluent cells were made quiescent at the G_0/G_1 phase of the cell cycle by changing the culture medium to DMEM containing 1% FCS. After 48 h of incubation, the medium was changed again to DMEM containing 5 μg/mL insulin and the cells were stimulated to initiate DNA synthesis by using different concentrations of peptides. Twelve hours later, [^{3}H-methyl]-thymidine was added and incorporation was continued for the next 12 h. Radioactivity incorporated into DNA was measured by a Beckman β-counter (Hewlet-Packard).[57] Each peptide was tested at least three times.

Affinity to Heparin−Sepharose Columns. The affinity was measured through the determination of the peptide ability to bind to a HEP−Sepharose column.[58] Peptide samples, ∼1.0 mg/mL in PBS containing 1.0 mg/mL bovine albumin serum, were loaded onto an HEP−Sepharose column (Pharmacia LKB Biotechnology AB) preequilibrated with 0.1 M NaCl in 0.01 M phosphate buffer, pH 7.2. Affinity chromatography was carried out using a linear gradient from 0.1 to 1.0 M NaCl in

0.01 M phosphate buffer, pH 7.2, in 24 min and a flow rate of 0.5 mL/min. Eluates were collected in fractions of 1.0 mL and analyzed by RP-HPLC in the same analytical instrument cited above. The affinity for HEP was inferred from the concentration of NaCl necessary for the elution.

Inhibitory Activity on the Binding of Human aFGF to Balb/c 3T3 Fibroblast Surface Receptors. The peptide ability to compete for the binding of ^{125}I-human aFGF to its receptor was measured as follows. The recombinant factor was labeled with ^{125}I (specific activity of 250 mCi/mL) using the chloramin T method described by Kan and co-workers.[59] The labeled protein was isolated by HEP−Sepharose chromatography. Balb/c 3T3 cells were seeded into a 24-well plate in DMEM/10% FCS. Subconfluent cells were incubated for 2.5 h at 4 °C with 18 ng/mL iodinated ^{125}I-human aFGF (specific activity of ∼31000−53000 cpm/ng), various concentrations of the peptides, 2 μg/mL of unlabeled aFGF dissolved in DMEM containing 20 mM Hepes (pH 7.2), and 10 mg/mL of bovine serum albumin. Cells were washed twice with cold phosphate-buffered saline (PBS) and solubilized with Triton X-100. The remaining iodinated human aFGF bound to the cells were quantified by γ-counting. Nonspecific binding was less than 10% of the total binding in all experiments performed in duplicate in at least three independent trials.

Circular Dichroism Measurements. The spectra have been recorded on a Jasco J-715 spectropolarimeter equipped with a Peltier apparatus for temperature control. The measurements were carried out at 20 °C in buffered aqueous solutions as a function of peptide concentration and pH or in the presence of different amounts of methanol (MeOH). Each spectrum was the average of four consecutive scans from 192 to 260 nm, followed by subtraction of the CD signal of the peptide-free solution. Peptide concentration was measured by ultraviolet absorbance using the extinction coefficient $\epsilon^{\mathrm{Trp}}_{280\mathrm{nm}} = 6309.57$. The curves are expressed as the mean residue molar ellipticity, $[\theta]_\lambda \times 10^{-3}$ (deg cm^2 dmol^{-1}).

Proton NMR Measurements. The two peptides were dissolved in a mixture of phosphate buffer solution, pH 6.0, and deuterated methanol (CD_3OH, 1:1 v/v) to yield a peptide concentration of 2−3 mM. ^{1}H NMR experiments were recorded on Bruker AMX 400 and DMX 500 spectrometers at 25 °C. The proton chemical shifts were referenced to the water signal located at 4.81 ppm.

Two-dimensional DQF-COSY,[60] clean-TOCSY[61] (mixing times of 15 and 80 ms), ROESY[62] (mixing times of 200 and 300 ms), and NOESY[63] (mixing time of 200 ms) experiments were recorded by standard techniques using presaturation of the water signal. Typically, 512 t_1 increments were acquired (32 or 64 scans/increment) with 2048 complex points in t_2, using the phase-sensitive mode.[64] Quadrature detection was achieved by hypercomplex data acquisition. Data were processed on a Silicon Graphics O2 workstation using the FELIX97 software package (Accelrys Inc., San Diego, CA). In general, a 90° phase-shifted squared-sine-bell function was used for apodization in both dimensions. The final matrices consisted of 2048 × 2048 real data points. Polynomial baseline correction was applied to the processed spectra wherever necessary.

Restraints Generation and Structure Calculation. The intensity of all nonoverlapping ROE cross-peaks has been evaluated by volume integration of the ROESY spectra. An internal calibration, based on a distance of 1.8 Å for well-defined geminal β-protons, was used to set the upper distance limits. The cross-peak intensities were thus grouped into different interatomic distance categories of 2.5, 3.0, 4.0, and 5.0 Å, and the lower bound was taken to be the sum of the van der Waals radii (1.8 Å) for the interacting protons. Pseudoatom corrections have been added to interproton distance restraints where necessary.[28] The ϕ dihedral angle restraints were derived from the $^3J_{\mathrm{HN}\alpha}$ coupling constants estimated either from 1D spectra or from the DQF-COSY spectra by measuring the separation of extrema in dispersive and absorptive plots of rows through cross-peaks.[65] The three-dimensional structures have been computed on a Silicon Graphics O2 workstation by means of either distance geometry and subsequent restrained energy minimization in the DISCOVER (Accelrys, San Diego, CA) CVFF force field[66] or the simulated annealing method[67] in the NMR Refine module of the INSIGHT II package (Accelrys, San Diego, CA), using the NMR-derived restraints. The quality of the final structures has been verified on the basis of the minimum number of ROE distance violations, ideal bond geometry, van der Waals contacts, and analysis of the ϕ and ψ dihedral angles in the Ramachandran plot. The degree of convergence of the structures was judged by examining the pairwise root-mean-square-deviation values for the backbone atoms in the region of interest.

Acknowledgment. This work was supported by grants from CNPq (doctoral scholarship to S.K.), FAPESP (Grant No. 98/1603-9 to M.T.M.M.), MIUR-2000, and CNR (Grant No. CNR 99.02608.CT04 to A.S.). The authors are grateful to Dr. H. A. Armelin for the use of the mitogenic activity measurement facility. The Centro Interfacoltà Misure of the University of Parma, Italy, and the Large Scale Facility for Biomolecular NMR of the University of Frankfurt, Germany, are acknowledged for the use of the CD, NMR, and computing facilities.

Appendix

Abbreviations. Ac, acetyl; aFGF, acidic fibroblast growth factor; bFGF, basic fibroblast growth factor; CVFF, consistent valence force field; CD, circular dichroism; COSY, correlation spectroscopy; DQF-COSY, double quantum filtered correlation spectroscopy; FGFs, fibroblast growth factors; FGFRs, fibroblast growth factors receptors; HS, heparan sulfate; HEP, heparin; MALDI-TOF, matrix-assisted laser desorption ionization time of flight; MeOH, methanol; NMR, nuclear magnetic resonance; NOESY, nuclear Overhauser enhancement spectroscopy; rmsd, root-mean-square deviation; ROE, rotating frame Overhauser effect; RP-HPLC, reversed-phase high-performance liquid chromatography; ROESY, rotating frame Overhauser effect spectroscopy; TFE, 2,2,2-trifluoroethanol; TOCSY, total correlation spectroscopy.

Footnote. The work was communicated in part in ref 43.

References

(1) Manetti, F.; Corelli, F.; Botta, M. Fibroblast growth factors and their inhibitors. *Curr. Pharm. Des.* **2000**, *6*, 1897−1924.
(2) Burgess, W. H.; Maciag, T. The heparin-binding (fibroblast growth factor) family of proteins. *Annu. Rev. Biochem.* **1989**, *58*, 575−606.
(3) Baird, A.; Klagsbrun, M. The fibroblast growth factor family. *Cancer Cells* **1990**, *3*, 239−243.
(4) Folkman, J.; Klagsbrun, M. Angiogenic factors. *Science* **1987**, *235*, 442−447.
(5) Jaye, M.; Schlessinger, J.; Dionne, C. A. Fibroblast growth factor receptor tyrosine kninases: molecular analysis and signal transduction. *Biochim. Biophys. Acta* **1992**, *1135*, 185−199.
(6) Ulrich, A.; Schlessinger, J. Signal transduction by receptors with tyrosine kinase activity. *Cell* **1990**, *61*, 203-212.
(7) McKeehan, W. L.; Wang, F.; Kan, M. The heparan sulfate-fibroblast growth factor family: diversity of structure and function. *Prog. Nucleic Acid Res. Mol. Biol.* **1998**, *59*, 135−173.
(8) Folkman, J.; Klagsbrun, M.; Sasse, J.; Wadzinski, M.; Ingber, D.; Vlodavsky, I. A heparin-binding angiogenic protein—basic fibroblast growth factor—is stored within basement-membrane. *Am. J. Pathol.* **1988**, *130*, 393−400.
(9) Vlodavsky, I. Extracellular sequestration and release of fibroblast growth factor: a regulatory mechanism? *Trends Biochem. Sci.* **1991**, *16*, 268−271.
(10) Gospodarowicz, D.; Cheng, J. Heparin protects basic and acidic fibroblast growth factors from inactivation. *J. Cell. Physiol.* **1986**, *128*, 475−484.

(11) Sommer, A.; Rifkin, D. B. Interaction of heparin with human basic fibroblast growth factor: protection of the angiogenic protein from proteolytic degradation by glucosaminoglycan. *J. Cell. Physiol.* **1989**, *138*, 215−220.
(12) Ornitz, D. M.; Herr, H. B.; Nilsson, M.; Westman, J.; Svahn, C. M.; Waksman, G. FGF binding and FGF receptor activation by synthetic heparan-derived di- and tri-saccharides. *Science* **1995**, *268*, 432−436.
(13) Casu, B.; Guerrini, M.; Naggi, A.; Perez, M.; Torri, G.; Ribatti, D.; Carminati, P.; Giannini, G.; Penco, S.; Pisano, C.; Belleri, M.; Rusnati, M.; Presta, M. Short Heparin sequences spaced by glycol-split uronate residues are antagonists of fibroblast growth factor 2 and angiogenesis inhibitors *Biochemistry* **2002**, *41*, 10519−10528
(14) Pantoliano, M. W.; Horlick, R. A.; Springer, B. A.; Van Dyk, D. E.; Tobery, T.; Wetmore, D. R.; Lear, J. D.; Nahapetian, A. T.; Bradley, J. D.; Sysk, W. P. Multivalent ligand−receptor binding interactions in the fibroblast growth factor system produce a cooperative growth factor and heparin mechanism for receptor dimerization. *Biochemistry* **1994**, *33*, 10229−19248.
(15) Springer, B. A.; Pantoliano, M. W.; Barbera, F. A.; Gunyulzu, P. L.; Thompson, L. D.; Herblin, W. F.; Rosenfeld, S. A.; Book, G. W. Identification and concerted function of two receptor binding surfaces on basic fibroblast growth factor required for mitogenesis. *J. Biol. Chem.* **1994**, *269*, 26879−26884.
(16) Oyama, S., Jr.; Miranda, M. T. M.; Kiyota, S.; Gambarini, A. G. Molecular modeling as a powerful tool for the mapping of fibroblast growth factor receptor-1 ligand binding determinants. *J. Mol. Model.* **1999**, *5*, 90−96.
(17) Di Gabrielli, A. D.; Lax, I.; Chen, D. I.; Svahn, C. M.; Jaye, M.; Schlessinger, J.; Hendrickson, W. A. Structure of a heparin-like biologically active dimmer of fibroblast growth factor. *Nature* **1998**, *393*, 812−817.
(18) Ventakaran, G.; Raman, R.; Sasisekharan, V.; Sasisekharan, R. Molecular characteristics of fibroblast growth factor−fibroblast growth factor receptor−heparin-like glycosaminoglycan complex. *Proc. Natl. Acad. Sci. U.S.A.* **1999**, *96*, 3658−3663.
(19) Huhtala, M. T.; Penkainen, O.; Johnson, M. S. A dimeric ternary complex of FGFR1, heparin and FGF-1 leads to an "electrostatic sandwich" model for heparin binding. *Structure* **1999**, *7*, 699−709.
(20) Stauber, D. J.; DiGabriele, A. D.; Hendrickson, W. A. Structural interaction of fibroblast growth factor receptor with its ligands. *Proc. Natl. Acad. Sci. U.S.A.* **2000**, *97*, 49−54.
(21) Kan, M.; Wang, F.; Xu, J.; Crabb, J. W.; Hou, J.; McKeehan, W. L. An essential heparin-binding domain in the fibroblast growth factor receptor kinase. *Science* **1993**, *259*, 1918−1921.
(22) Blaber, M.; DiSalvo, J.; Thomas, K. A. X-ray crystal structure of human acidic fibroblast growth factor. *Biochemistry* **1996**, *35*, 2086−2094.
(23) Ogura, K.; Nagata, K.; Hatanaka, H.; Habuchi, H.; Kimata, K.; Tate, S.-I.; Ravera, W. R.; Jaye, M.; Schlessinger, J.; Inagaki, F. Solution structure of human acidic fibroblast growth factor and interaction with heparin-derived hexasaccharide. *J. Biomol. NMR* **1999**, *13*, 11−24.
(24) Reich-Slottky, R.; Shaoul, E.; Berman, B.; Graziani, G.; Ron, D. Chimeric molecules between keratinocyte growth factor and basic fibroblast growth factor define domains that confer receptor binding specificity. *J. Biol. Chem.* **1995**, *270*, 29813−29818.
(25) Pellegrini, L.; Burke, D. F.; von Delft, F.; Mulloy, B.; Blundell, T. L. Crystal structure of fibroblast growth factor receptor ectodomain bound to ligand and heparin. *Nature* **2000**, *407*, 1029−1034.
(26) Oyama, S., Jr.; Miranda, M. T. M.; Toma, I. N.; Viviani, W.; Gambarinin, A. Mitogenic activity of peptides related to the sequence of human fibroblast growth factor-1. *Biochem. Mol. Biol. Int.* **1996**, *39*, 1237−1244.
(27) Brych, S. R.; Blaber, S. I.; Logan, T. M.; Blaber, M. Structure and stability effects of mutations designed to increase the primary sequence symmetry within the core region of a b-trefoil. *Protein Sci.* **2001**, *10*, 2587−2599.
(28) Wüthrich, K. *NMR of Proteins and Nucleic Acids*; John Wiley & Sons: New York, 1986.
(29) Kelly, L. A.; Gardner, S. P.; Sutcliffe, M. J. An automated approach for clustering an ensemble of NMR-derived structures into conformationally related subfamilies. *Protein Eng.* **1996**, *9*, 1063−1065.
(30) Moult, J.; Melamud, E. From fold to function. *Curr. Opin. Struct. Biol.* **2000**, *10*, 384−389.
(31) Sanz, J. M.; Jiménez, M. A.; Giméenez-Gallego, G. Hints of nonhierarchical folding of acidic fibroblast growth factor. *Biochemistry* **2002**, *41*, 1923−1933.
(32) Chung, D. A.; Zuiderweg, E. R. P.; Fowler, C. B.; Soyer, O. S.; Mosberg, H. I.; Neubig, R. R. NMR structure of the second intracellular loop of the α2A-adrenergic receptor: evidence for a novel cytoplasmic helix. *Biochemistry* **2002**, *41*, 3596−3604.
(33) Naider, F.; Arshava, B.; Ding, F-X.; Arevalo, E.; Becker, J. M. Peptide fragments as models to study the structure of a G-protein coupled receptor: the alfa-factor receptor of *Sacharomices cerevisiae*. *Biopolymers* **2001**, *60*, 334−350.
(34) Chamberlin, S. G.; Sargood, K. J.; Richter, A.; Mellor, J. M.; Anderson, D. W.; Richards, N. G. J.; Turner, D. L.; Sharma, R. P.; Alexander, P.; Davies, D. E. Constrained peptide analogues of transforming growth factor-a residues cysteine 21−32 are mitogenically active. *J. Biol. Chem.* **1995**, *270*, 21062−21067.
(35) Rizo, J.; Sutton, R. B.; Breslau, J.; Koerber, S. C.; Porter, J.; Hagler, A. T.; Rivier, J. E.; Gierasch, L. M. A novel conformation in a highly potent, constrained gonadotropin-releasing hormone antagonist. *J. Am. Chem. Soc.* **1996**, *118*, 970−976.
(36) Schwyzer, R. 100 years lock-and-key concept: are peptide keys shaped and guided to their receptors by target cell membrane? *Biopolymers* **1995**, *37*, 5−16.
(37) Ruan, K.-H.; So, S.-P.; Wu, J.; Huang, A.; Kung, J. Solution structure of the second extracellular loop of human thromboxane A2 receptor. *Biochemistry* **2001**, *40*, 275−280.
(38) Nicastro, G.; Peri, F.; Franzoni, L.; de Chiara, C.; Sartor, G.; Spisni, A. Conformational Features of a Synthetic Model of the First Extracellular Loop of the Angiotensin II AT1A Receptor. *J. Pept. Sci.*, in press.
(39) Bottaro, D. P.; Fortney, E.; Rubin, J. S.; Aaronson, S. A. A keratinocyte growth factor receptor-derived peptide antagonist identifies part of the ligand binding site. *J. Biol. Chem.* **1993**, *268*, 9180−9183.
(40) Yayon, A.; Aziezer, D.; Safran, M.; Gross, J. L.; Heldmann, Y.; Cabilly, S.; Givol, D.; Katchalski-Ktzir, E. Isolation of peptides that inhibit binding of basic fibroblast growth factor to its receptor from a random phage-epitope library. *Proc. Natl. Acad. Sci. U.S.A.* **1993**, *90*, 10643−10647.
(41) Wong, P.; Hampton, B.; Szylobryt, E.; Gallagher, A. M.; Jaye, M.; Burgess, W. H. Analysis of putative heparin-binding domains of fibroblast growth factor-1. *J. Biol. Chem.* **1995**, *270*, 25805−25811
(42) Fromm, J. R.; Hileman, H. E.; Weiler, J. M.; Linhardt, R. J. Interaction of fibroblast growth factor-1 and related peptides with heparan sulfate and its oligosaccharides. *Arch. Biochem. Biophys.* **1997**, *346*, 252−262.
(43) Kiyota, S.; Gambarini, A. G.; Viviani, W.; Oyama, S., Jr.; Toma, I. N.; Sykes, B. D.; Miranda, M. T. M. New synthetic peptides derived from human fibroblast growth factor-1: search for agonists and inhibitors. In *Peptides: Frontiers of Peptide Science*; Proceedings of the 15th American Peptide Symposium, Nashville, TN, June 14−19, 1999; Tam, J. P., Kaumaya, P. T. P., Eds.; ESCOM/Kluwer: Dordrecht, The Netherlands, 1999; pp 641−642.
(44) Flaumenhaft, R.; Moscatelli, D.; Rifkin, D. B. Heparin and heparan sulfate increase the radius of diffusion and action of basic fibroblast growth factor. *J. Cell. Biol.* **1990**, *111*, 1651−1659.
(45) Thompson, L. D.; Pantoliano, M. W.; Springer, B. A. Energetic characterization of the basic fibroblast growth factor−heparin interaction: identification of the heparin binding domain. *Biochemistry* **1994**, *33*, 3831−3840.
(46) Ballinger, M. D.; Venkatakrishna, S.; Forrest, L. D.; Deuter-Reinhard, M.; Doyle, L. V.; Wang, J.-X.; Panganiban-Lustan, L.; Stratton, J. R.; Apell, G.; Winter, J. A.; Doyle, M. V.; Rosenberg, S.; Kavanaugh, W. M. Semirational design of a potent, artifical agonist of fibroblast growth factor receptors. *Nat. Biotechnol.* **1999**, *17*, 1199−1204.
(47) DeLano, W. L.; Ultsch, M. H.; de Vos, A. M.; Wells, J. A. Convergent solutions to binding at a protein−protein interface. *Science* **2000**, *287*, 1279−1282.
(48) Hu, Z.; Ma, B.; Wolfson, H.; Nussinov, R. Conservation of polar residues as hot spots at protein interfaces. *Proteins: Struct., Funct., Genet.* **2000**, *39*, 331−342.
(49) Zhu, Z.; Komiya, H.; Chirino, A.; Faham, S.; Fox, G. M.; Arakawa, T. A. A.; Hsu, B. T.; Rees, D. C. Three-dimensional structures of acidic and basic fibroblast growth factors. *Science* **1991**, *251*, 90−93.
(50) Plotnikov, A. N.; Schlessinger, J.; Hubbard, S. R.; Mohammadi, M. Structural basis for FGF receptor dimerization and activation. *Cell* **1999**, *98*, 641−650.
(51) Murzin, A. G.; Lesk, A. M.; Chothia, C. b-Trefoil fold−patterns of structures and sequence in the Kunitz inhibitors, intrleukins-1b and 1a and fibroblast growth factors. *J. Mol. Biol.* **1992**, *233*, 531−543.
(52) Faham, S.; Hileman, R. E.; Fromm, J. R.; Linhardt, R. J.; Rees, D. C. Heparin structure and interactions with basic fibroblast growth factor. *Science* **1996**, *271*, 1116−1120.
(53) Pineda-Lucena, A.; Jiménez, M. A.; Lozano, R. M.; Nielo, J. L.; Santoro, J.; Rico, M.; Giménez-Gallego, G. Three-dimensional structure of acidic fibroblast growth factor in solution: effects of binding to a heparin functional analog. *J. Mol. Biol.* **1996**, *264*, 162−178.

(54) Varanda, L. M.; Miranda, M. T. M. Solid-phase peptide synthesis at elevated temperatures: a search for an optimized synthesis condition of unsulfated cholecystokinin-12. *J. Pept. Res.* **1997**, *50*, 102−108.
(55) Misicka, A.; Hruby, V. J. Optimization of disulfide bond formation. *Pol. J. Chem.* **1994**, *68*, 893−99.
(56) Miranda, M. T. M.; Liddle, R. A.; Rivier, J. E. Synthesis of human CCK 26−33 and CCK-33 related analogs on 2,4-DMBHA and TMBHA. *J. Med. Chem.* **1993**, *36*, 1681−1688.
(57) Armelin, H. A. Pituitary extracts and steroid hormones in the control of 3T3 cell growth. *Proc. Natl. Acad. Sci. U.S.A.* **1973**, *70*, 2702−2706.
(58) Shing, Y.; Folkman, J.; Sullivan; R.; Butterfield, C.; Murray, J.,; Klagsbrun, M. Heparin-affinity: purification of a tumor derived capillary endothelial cell growth factor. *Science* **1984**, *223*, 1296−1298.
(59) Kan, M.; Shi, E. G.; Mckeehan, W. L. Identification and assay of fibroblast growth factor receptors. *Methods Enzymol.* **1991**, *198*, 159−171.
(60) Rance, M.; Sorensen, O. W.; Bodenhausen, G.; Wagner, G.; Ernst, R. R.; Wüthrich, K. Improved spectral resolution in COSY ^{1}H NMR spectra of proteins via double quantum filtering. *Biochem. Biophys. Res. Commun.* **1983**, *117*, 479−485.
(61) Davis, D. G.; Bax, A. Assignment of complex proton NMR spectra via two-dimensional homonuclear Hartmann−Hahn spectroscopy. *J. Am. Chem. Soc.* **1985**, *107*, 2820−2821.
(62) Bax, A.; Davis, D. G. Practical aspects of two-dimensional transverse NOE spectroscopy. *J. Magn. Reson.* **1985**, *63*, 207−213.
(63) Kumar, A.; Ernst, R. R.; Wüthrich, K. A two-dimensional nuclear Overhauser enhancement (2D NOE) experiment for the elucidation of complete proton−proton cross-relaxation networks in biological macromolecules. *Biochem. Biophys. Res. Commun.* **1980**, *95*, 1−6.
(64) States, D. J.; Haberkorn, R. A.; Ruben, D. J. A two-dimensional nuclear Overhauser experiment with pure absorption phase in four quadrants. *J. Magn. Res.* **1982**, *48*, 286−292.
(65) Kim, Y.; Prestegard, J. H. Measurement of vicinal couplings from cross peaks in COSY spectra. *J. Magn. Res.* **1989**, *84*, 9−13.
(66) Dauber-Osguthorpe, P.; Roberts, V. A.; Osguthorpe, D. J.; Wolff, D. J.; Genest, M.; Hagler, A. T. Structure and energetics of ligand binding to proteins: *E. col*i dihydrofolate reductase−trimethoprim, a drug−receptor system. *Proteins: Struct., Funct., Genet.* **1988**, *4*, 31−47.
(67) Nilges, M.; Clore, G. M.; Gronenborn, A. Determination of three-dimensional structures of proteins from interproton distance data by dynamical simulated annealing from a random array of atoms. Circumventing problems associated with folding. *FEBS Lett.* **1998**, *239*, 129−136.

JM020543E